Some problems of simulation of nonisothermal adsorption

[a]E. KOSSACZKÝ, [b]T. KAPUSTA, and [a]D. BOBOK

[a]*Department of Chemical Engineering, Slovak Technical University, CS-812 37 Bratislava*

[b]*Juraj Dimitrov Chemical Works, CS-836 05 Bratislava*

Received 1 March 1984

Accepted for publication 22 July 1985

An equilibrium model of nonisothermal adsorption and a model comprising the resistance against mass transfer in the solid phase have been designed. The mathematical relationships valid for the models have been transformed in dimensionless form and used for disclosing the influence of heat accumulation, heat loss, and mass transfer in the solid phase on the course of nonadiabatic and nonisothermal adsorption. It has been revealed that heat accumulation, heat loss, and solid-phase mass transfer resistance have significant influence on attaining good agreement of the calculation with the experiment carried out under laboratory conditions, especially for systems with high adsorption heat and relatively high concentration of adsorptive in the feed gas.

Разработана равновесная модель неизотермической адсорбции и модель, учитывающая сопротивление переносу вещества в твердой фазе. Математические уравнения моделей, приведенные в безразмерный вид, были использованы для определения влияния аккумуляции тепла, потерь тепла и переноса вещества в твердой фазе на ход неадиабатической и неизотермической адсорбции. Оказалось, что аккумуляция тепла, потери тепла и сопротивление переносу вещества в твердой фазе оказывают решающее влияние на достижение удовлетворительной согласованности между рассчетом и экспериментом проводимым в лабораторных условиях, в особенности, для систем с большой теплотой адсорбции и относительно высокой концентрацией адсорбируемого вещества в сырье.

In spite of a great number of papers dealing with adiabatic and nonisothermal sorption, we cannot think that this separation process has been mastered. Most mathematical models as well as experimental investigations have been concerned with systems in which the thermal effects are not very conspicuous.

The solution of nonisothermal sorption consists in designing a system of partial differential equations describing the distribution of concentration of adsorptive, adsorbate, and temperature in an adsorber during adsorption. The equilibrium relationship and initial and boundary conditions are to be attributed to the system

of equations. The analytical solution of this system of equations is not hitherto known and the numerical solution is only a particular solution for given initial and boundary conditions. The aim in designing a physical and mathematical model is to obtain the possibly simplest system of equations which could adequately describe nonisothermal sorption.

The equilibrium model with plug flow is the simplest one. Even the calculation according to this model the results of which have the character of the first approximation is rather time-consuming, especially if the phase equilibrium is described by complex relation. The need of computing time significantly increases if the mathematical model of equilibrium adsorption is extended by kinetic relationships of the mass and heat transfer between the phases and by the terms expressing the heat exchange between the system and environment (nonadiabatic adsorption, nonisothermal adsorption).

This paper deals with the influence of the generated adsorption heat on the course of break-through curve and shape of temperature profiles in the adsorbent bed modelled as a nonisothermal and nonadiabatic system.

Theoretical

For deriving a model of nonisothermal sorption we assume a cylindrical adsorber filled with granulated adsorbent in which the adsorptive is trapped from the stream of indifferent gas. Further assumptions on which the model is based may be summarized in these items.

a) Both phases, *i.e.* liquid and solid, are regarded as continua existing besides each other in continuous phase contact on the interface the surface area of which related to the volume unit of adsorber is equal to the surface solid particles in a volume unit of the adsorbent.

b) The liquid phase flows through the bed in a straight-line manner without back mixing with a constant velocity along the column.

c) The concentration and temperature profiles in both phases are continuous functions of position and time and do not depend on the position of an individual particle in the bed.

d) The liquid phase fills up a constant part of the volume of adsorbent bed and its density as well as bulk density of adsorbent bed does not change with position and time.

e) Only one component is adsorbed from the stream of indifferent gas.

f) The material characteristics of the liquid and solid phase are independent of temperature and concentration and constant in the investigated temperature and concentration range.

As the derivation of the model as well as the discussion about the assumptions have been presented in paper [1], we are going to give only the resulting forms of the equations.

Material balance

$$\varrho_b\left(\frac{\partial x}{\partial t}\right)_z + \frac{\varrho_2 \varepsilon}{M_2}\left(\frac{\partial Y_g}{\partial t}\right)_z + \dot{n}_2\left(\frac{\partial Y_g}{\partial z}\right)_t = 0 \tag{1}$$

Enthalpic balance

$$-(-\Delta H)\varrho_b\left(\frac{\partial x}{\partial t}\right)_z + \left\{\varrho_b c_{pb} + \varrho_g c_{pg}\varepsilon + v\left[\left(\frac{d_2}{d_1}\right)^2 - 1\right]\varrho_s c_{ps}\right\} \cdot \left(\frac{\partial T_g}{\partial t}\right)_z +$$

$$+ c_{pg}\bar{M}\dot{n}_2\left[(1+Y_g)\left(\frac{\partial T_g}{\partial z}\right)_t + T_g\left(\frac{\partial Y_g}{\partial z}\right)_t\right] + \frac{4k_t}{d_1}(T_g - T_f) = 0 \tag{2}$$

As the equilibrium relation we used the modified Langmuir equation [2]

$$x^* = A_1 \exp(-B_1 T_g)\frac{Y_g \exp(R_1/T_g)}{D_1\sqrt{T_g} + [D_1\sqrt{T_g} + \exp(R_1/T_g)]Y_g} \tag{3}$$

The mass transfer in a solid particle was described phenomenologically as a mass transfer in a fictitious film of the solid phase [3, 4]

$$\frac{\partial x}{\partial t} = K_s(x^* - x) \tag{4}$$

The given systems of equations is connected with initial and boundary conditions

$$Y_g(0, z) = Y_{gi};\ T_g(0, z) = T_{gi};\ x(0, z) = x_i$$

$$Y_g(t, 0) = Y_{g0};\ T_g(t, 0) = T_{g0} \text{ for } t > 0 \tag{5}$$

In order to obtain a certain generalization of the results, we have transformed the differential equations into the dimensionless form. This procedure results in a decrease in number of the parameters occurring in the equations. The numerical solution of these equations complies with all particular values of physical parameters provided all dimensionless parameters derived from them have equal values. The transformation of eqns (*1*—*5*) into the dimensionless form by the procedure presented in publication [5] is thoroughly described in [1].

The resulting form of the dimensionless equations for equilibrium model derived from eqns (*1*—*3*) and (*5*) is

$$\left(\frac{\partial Y}{\partial \Theta}\right) = \left[\mathrm{AY}\cdot\left(\frac{\partial Y}{\partial Z}\right) + \mathrm{BY}\cdot\left(\frac{\partial Y}{\partial Z}\right) + \mathrm{CY}\cdot(T - \mathrm{TF})\right]/\mathrm{AB} \tag{6}$$

$$\left(\frac{\partial T}{\partial \Theta}\right)=\left[\mathrm{AT}\cdot\left(\frac{\partial Y}{\partial Z}\right)+\mathrm{BT}\cdot\left(\frac{\partial T}{\partial Z}\right)+\mathrm{CT}\cdot(T-\mathrm{TF})\right]/\mathrm{AB} \tag{7}$$

where $\mathrm{AT}=\alpha\cdot\mathrm{DH}+T(\alpha+E\cdot\mathrm{R2})\cdot\mathrm{CP}\cdot(YM(\mathrm{CO_2})/M_2+1)/(Y+1)$

$\mathrm{BT}=(\alpha+E\cdot\mathrm{R2})\cdot\mathrm{CP}\cdot(YM(\mathrm{CO_2})/M_2+1)$

$\mathrm{CT}=\mathrm{KT}\cdot(\alpha+E\cdot\mathrm{R2})$

$\mathrm{AY}=\beta\mathrm{T}\cdot\mathrm{CP}\cdot(YM(\mathrm{CO_2})/M_2+1)/(Y+1)-\mathrm{ZC}+\beta\cdot\mathrm{DH}$

$\mathrm{BY}=\beta\cdot\mathrm{CP}\cdot(YM(\mathrm{CO_2})/M_2+1)$

$\mathrm{CY}=\beta\cdot\mathrm{KT}$

$\mathrm{AB}=(\alpha+E\cdot\mathrm{R2})(\mathrm{ZC}-\beta\cdot\mathrm{DH})+\alpha\beta\cdot\mathrm{DH}$

$$\alpha=A\exp(-\mathrm{BT})\frac{D\sqrt{T}\exp(R/T)}{\{D\sqrt{T}+[D\sqrt{T}+\exp(R/T)]Y\}^2}$$

$$\beta=-A\exp(-\mathrm{BT})\frac{\exp(R/T)Y}{D\sqrt{T}+[D\sqrt{T}+\exp(R/T)]Y}\cdot$$

$$\cdot\left[B+\frac{D\sqrt{T}(1+Y)(2R+T)}{\{D\sqrt{T}+[D\sqrt{T}+\exp(R/T)]Y\}2T^2}\right]$$

$$\mathrm{DH}=\frac{-(\Delta H)}{c_{p\mathrm{b}}T_{g0}M_2},\quad \mathrm{RS}=\varrho_s/\varrho_\mathrm{b},\quad \Theta=\frac{t\dot{n}_2M_2}{\varrho_\mathrm{b}z_0}$$

$$T=\frac{T_g}{T_{g0}},\quad \mathrm{KT}=\frac{4k_tz_0}{M_2\dot{n}_2d_1c_{p\mathrm{b}}},\quad X=xM_2$$

$$D_2=d_2/d_1,\quad \mathrm{TF}=\frac{T_f}{T_{g0}},\quad Y=\frac{Y_g}{Y_{g0}}$$

$$E=\varepsilon,\quad Z=\frac{z}{z_0},\quad \mathrm{ZC}=1+E\cdot\mathrm{RO}\cdot\mathrm{CP}+v(D_2^2-1)\cdot\mathrm{RS}\cdot\mathrm{CPS}$$

$$\mathrm{R2}=\frac{\varrho_2}{\varrho_\mathrm{b}},\quad \mathrm{CP}=\frac{c_{pg}}{c_{p\mathrm{b}}},\quad \mathrm{RO}=\frac{\varrho_2}{\varrho_\mathrm{b}}$$

$$\mathrm{CPS}=\frac{c_{ps}}{c_{p\mathrm{b}}},\quad A=A_1M_2,\quad B=B_1T_{g0}$$

$$R=\frac{R_1}{T_{g0}},\quad D=D_1\sqrt{T_{g0}}$$

The initial and boundary conditions in the dimensionless form are as follows

$$Y(0,Z)=Y_{gi},\quad T(0,Z)=T_{gi}/T_{g0},\quad X(0,Z)=x_iM_2$$

$$Y(\Theta,0)=Y_{g0},\ T(\Theta,0)=T_{g0}/T_{g0}=1\qquad \text{for } \Theta>0 \tag{8}$$

The resulting form of the dimensionless equations for the model involving the resistance against mass transfer in the solid phase which has been derived from eqns (*1*—*5*) may be written as follows

$$E \cdot \mathrm{R2} \cdot \left(\frac{\partial Y}{\partial \Theta}\right) + \left(\frac{\partial Y}{\partial Z}\right) + \left(\frac{\partial X}{\partial \Theta}\right) = 0 \tag{9}$$

$$\mathrm{ZA} \cdot \left(\frac{\partial T}{\partial Z}\right) + \mathrm{ZB} \cdot \left(\frac{\partial Y}{\partial Z}\right) + \mathrm{ZC} \cdot \left(\frac{\partial T}{\partial \Theta}\right) + \mathrm{KT} \cdot (T - \mathrm{TF}) - \\ - \mathrm{DH} \cdot \left(\frac{\partial X}{\partial \Theta}\right) = 0 \tag{10}$$

$$\left(\frac{\partial X}{\partial \Theta}\right) = \mathrm{KS}(X^* - X) \tag{11}$$

$$X^* = A \exp(-\mathrm{BT}) \frac{\exp(R/T)Y}{D\sqrt{T} + [D\sqrt{T} + \exp(R/T)]Y} \tag{12}$$

where $\mathrm{ZA} = \mathrm{CP} \cdot (YM(\mathrm{CO_2})/M_2 + 1)$
$\mathrm{ZB} = \mathrm{CP} \cdot T(YM(\mathrm{CO_2})/M_2 + 1)/(Y + 1)$
$\mathrm{ZC} = 1 + E \cdot \mathrm{RO} \cdot \mathrm{CP} + v(D_2^2 - 1) \cdot \mathrm{RS} \cdot \mathrm{CPS}$

$$\mathrm{KS} = \frac{15 D_{\mathrm{ef}} \varrho_b z_0}{r^2 \dot{n}_2 M_2}; \quad D_{\mathrm{ef}} = a\, \mathrm{e}^{-(b/T_g)} \text{ [1]}$$

Other dimensionless quantities as well as the initial and boundary conditions have been given in the description of the equilibrium model.

Experimental

Molecular sieve Calsit 5, product of the Research Institute of Petroleum and Hydrocarbon Gases, Bratislava, balls of 2—3 mm diameter, content of binding agent 20 mass %, mineral density 2858 kg m^{-3}, crystallographic density 1777 kg m^{-3}, particle density 1148 kg m^{-3}, bulk density 721 kg m^{-3}. Chemical composition (w_i/%): SiO_2 41.8, Fe_2O_3 1.4, MgO 0.5, Al_2O_3 37.4, CaO 16.3, Na_2O 2.2. Carbon dioxide taken from pressure flasks was dried in a bed of molecular sieve of the type A. The content of CO_2 was 99.9 mole %. Nitrogen of electric bulb industry was used after its purification. The oxygen rest was trapped by chemisorption on the Ronge copper and the moisture was removed by adsorption on molecular sieve of the type A. The laboratory equipment and measuring procedure were, in principle, identical with that one described in literature [6]. The experiment in which a temperature isolation of foamed polyuretane was used is denoted as quasi-adiabatic and the experiment performed without isolation is regarded as nonisothermal. The conditions of the experiments are given in Table 1.

Table 1

Conditions of experiments

Flow $\dot{n}$/kmol m^{-2} h^{-1}		Y_0	Y_i	T_0	T_i	T_m	p_b	π	m_{Ms}	z_0	Isolation
N_2	CO_2			K	K	K	kPa	kPa	kg	m	
22.0	4.4	0.25	0	303	303	299	101.3	128.0	0.523	0.685	present
40.9	8.2	0.25	0	303	303	296	99.8	126.5	0.523	0.685	absent

Results and discussion

The Runge—Kutta integration method of the fourth order was used for numerical solution of both models by means of a computer. The equations were transformed from partial differential equations into differential difference equations by using reverse difference instead of derivation with respect to length (eqns (*6*) and (*7*)) or instead of derivation with respect to time (eqns (*9*) and (*10*)). The values of dimensionless parameters of the adsorption system necessary for numerical calculations are given in Tables 2 and 3.

In numerical simulation we attempted to investigate the influence of heat loss from adsorber during adsorption as well as the influence of heat accumulation in the walls and isolation of adsorber on the course of adsorption. The heat loss coefficient at nonisolated adsorber was estimated by the equation

$$k_t = \frac{1}{\frac{\delta_s}{\lambda_s} + \frac{1}{\alpha_K}} \tag{13}$$

where δ_s is wall width of the adsorber, λ_s stands for thermal conductivity of glass (walls of adsorber), and α_K is the combined coefficient of heat transfer by radiation and convection [7]

$$\alpha_K = \alpha_p + \alpha_r \tag{14}$$

the value of which may be appraised from the empirical equation [7]

$$\alpha_K = (8.4 + 0.06(\vartheta_w - \vartheta_f)) \times 4.1868 \tag{15}$$

Computing the heat losses from an isolated adsorber we have considered only the heat conduction because other resistance against heat transfer may be neglected in comparison with the effect of isolation. Thus we can write

$$k_t = \frac{\lambda_i}{\delta_i} \tag{16}$$

where δ_i and λ_i are width of isolation and thermal conductivity of isolation, respectively. However, the coefficients of heat transfer thus appraised represent only informative values. Their contribution to precision of simulation is also reduced by the fact that they are regarded as constant quantities which are independent of temperature in the course of thermally nonsteady state process.

Table 2

Values of dimensionless parameters for equilibrium model

$E \cdot R2 \cdot 10^4$	DH	ZC	KT	D	Isolation	Figures	Denotation in figures
7.437	5.382	1.76	0.5337	14 752	present	1, 2	-.-.-.-.-.-.
7.437	5.382	2.25	0.5337	14 752	present	1, 2	.....
7.437	5.382	3.00	0.5337	14 752	present	1, 2	--------
7.362	5.382	1.57	0.7200	14 926	absent	3, 4	--------
7.362	5.382	1.57	3.0000	14 926	absent	3, 4	-.-.-.-.-.-.

Table 3

Values of dimensionless parameters for the model including mass transfer in the solid phase

$E \cdot R2 \cdot 10^4$	DH	ZC	KT	D	KS	Isolation	Figures	Denotation in figures
7.437	5.382	2.00	0.5337	14 752	$5.0 \times 10^7\ e^{-(15/T)}$	present	5, 6	-.-.-.-.-.-.
7.437	5.382	2.25	0.5337	14 752	$5.0 \times 10^7\ e^{-(15/T)}$	present	5, 6	.....
7.437	5.382	3.00	0.5337	14 752	$2.5 \times 10^6\ e^{-(11.5/T)}$	present	5, 6	--------
7.362	5.382	1.57	3.0000	14 926	$1.3 \times 10^6\ e^{-(11.5/T)}$	absent	7, 8	-.-.-.-.-.-
7.362	5.382	1.81	3.2700	14 926	$2.5 \times 10^6\ e^{-(11.5/T)}$	absent	7, 8	--------
7.362	5.382	1.81	3.2700	14 926	$1.3 \times 10^6\ e^{-(11.5/T)}$	absent	7, 8	.....

Values of dimensionless constants in equilibrium relationship $A = 0.1837168$, $B = 0.5903795$, $R = 13.2826$.
Value of parameter CP = 1.098; dimensionless temporal integration step — 10^{-3}; dimensionless length increment — 2×10^{-2}.

The estimation of heat accumulation in isolation brings the problem of correct determination of the heat capacity of isolation as well as its dependence on temperature. Other difficulties are connected with the determination of the degree of foaming and homogeneity of polyurethane isolation in the radial and axial direction. In order to avoid these difficulties, we put forward the concept of hypothetical isolation the heat capacity of which is the $(v-1)$th multiple of the heat capacity of adsorber wall

$$v = 1 + (d_3^2 - d_2^2)c_{pi}\varrho_i/(d_2^2 - d_1^2)c_{ps}\varrho_s \tag{17}$$

The course of break-through curve in an experiment for which the isolation of foamed polyurethane was used is depicted by full line in Fig. 1. Other three lines in Fig. 1 are the break-through curves calculated for different values of heat accumulation in hypothetical isolation (v) according to the equilibrium model. As obvious from Fig. 1, the break-through curves shift to the right hand on the axis of

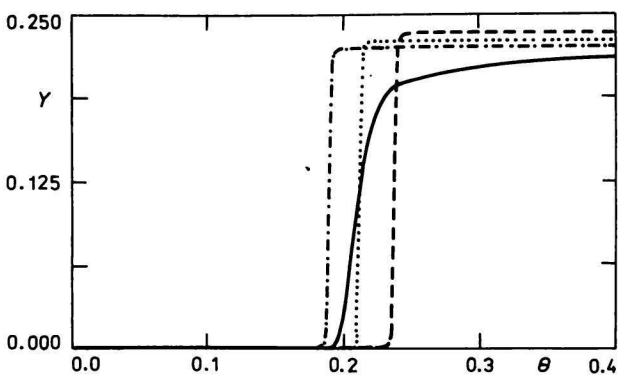

Fig. 1. Break-through curves; full line — experiment with isolated adsorber; dashed lines — calculated according to equilibrium model for different values of the parameter of heat accumulation (given in Table 2).

dimensionless time with increasing value of heat accumulation while the concentration plateau shifts to higher values on the axis of relative fraction. These shifts are evidently connected with the mean temperature of adsorbent in adsorber which affects the dynamic capacity of adsorbent by means of the equilibrium relation. The full lines in Fig. 2 represent the temperature course in 1/3, 2/3, and 3/3 of the length of adsorber while other curves give the calculated course of temperature in

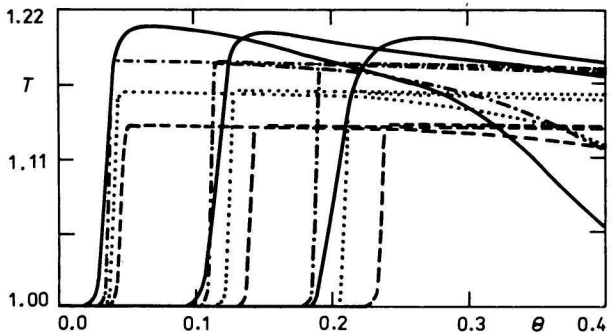

Fig. 2. Course of temperature in the first, second, and third part of adsorber; full lines — experiment with isolated adsorber; dashed lines — calculated according to equilibrium model for different values of the parameter of heat accumulation (given in Table 2).

these points of adsorber. The calculated temperature dependence is always below the measured one, which must be due to the fact that the experimental temperatures were measured along the axis of adsorber by means of glass probes and the radial temperature gradient was not taken into account in deriving the model. A comparison of the calculated temperature curves in Fig. 2 and the mean temperatures in adsorber appraised from those curves suggest that the mean temperature in adsorber determines the break-through point. Fig. 2 also shows that the rate of temperature decrease in the first third of adsorber is smaller for higher values of the accumulation parameter.

The course of break-through curve for the experiment performed under nonisothermal conditions (adsorber without isolation) is depicted by full line in Fig. 3. Other two curves in Fig. 3 are the break-through curves calculated according to the equilibrium model for different values of the heat loss parameter. An increase in value of this parameter results in shifting the break-through curve to the right-hand side and the concentration plateau to lower values on the composition axis while the slope of this part of break-through curve increases. The height of break-through curve is evidently determined by the rate of supplementary saturation of adsorbent by adsorbate which depends on temperature of the adsorbent and degree of its saturation. On the basis of comparison of the rates of temperature decrease according to Fig. 2 and Fig. 4, we may appraise the instantaneous rates of supplementary saturation for different conditions of the process. Fig. 2 shows that the highest instantaneous rate of supplementary saturation appears at the lowest value of the parameter of heat accumulation and thus the position of the concentration plateau on the break-through curve is lower. Similarly, it results

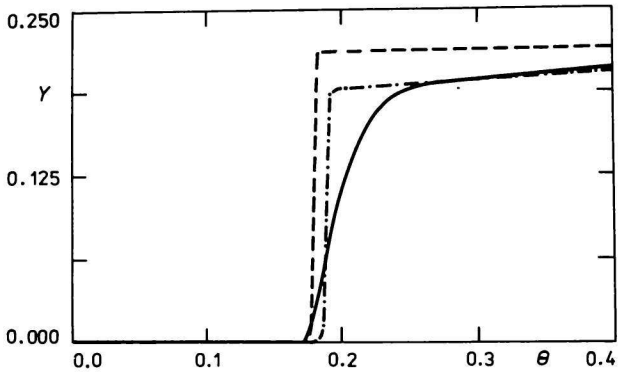

Fig. 3. Break-through curves; full line — experiment with nonisolated adsorber; dashed lines — calculated according to equilibrium model for different values of the parameter of heat loss (given in Table 2).

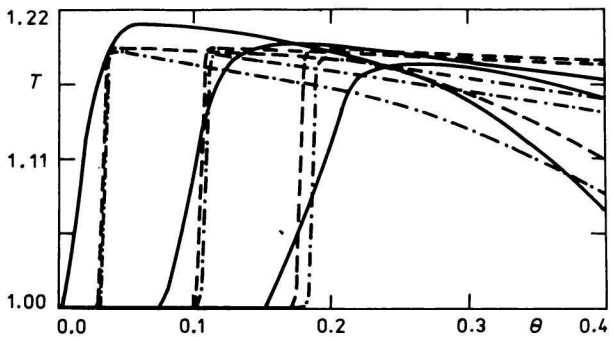

Fig. 4. Course of temperature in the first, second, and third part of adsorber; full lines — experiment with nonisolated adsorber; dashed lines — calculated according to equilibrium model for different values of the parameter of heat loss (given in Table 2).

from Fig. 4 that the instantaneous rate of supplementary saturation for higher value of the parameter of heat loss is initially higher but it decreases in further progress of adsorption more rapidly than it does for lower value of the parameter of heat loss for which the rate of supplementary saturation is initially lower.

Because of high values of the molar flow in the nonequilibrium model (Figs. 5—8), we took into consideration only the resistance against mass transfer in the solid phase as expressed by eqn (*4*). For the experiment performed with isolation (Figs. 5 and 6) the measured break-through curves and temperature profiles are represented by full lines and the calculated ones by dashed lines. The course of these functions enables us to make equal conclusions as stated in connection with the equilibrium model.

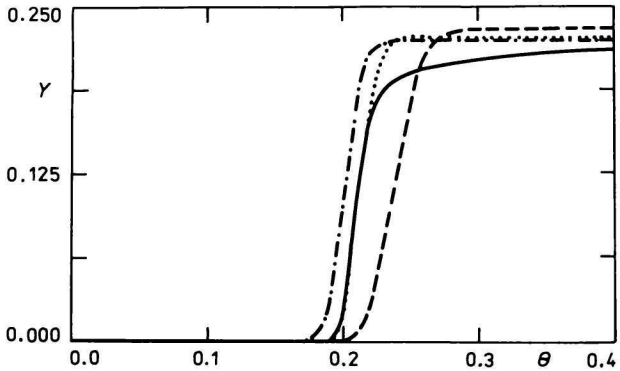

Fig. 5. Break-through curves; full line — experiment with isolated adsorber; dashed lines — calculated according to nonequilibrium model for different values of the parameter of heat accumulation and parameter KS of the rate equation (*11*) (given in Table 3).

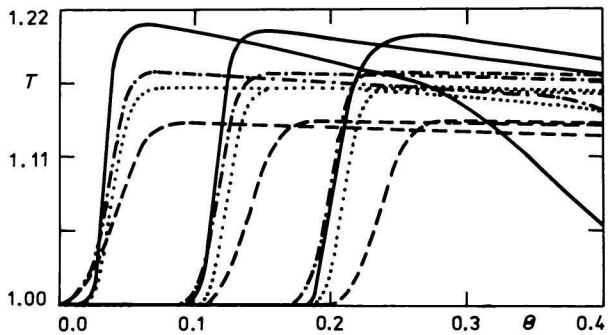

Fig. 6. Course of temperature in the first, second, and third part of adsorber; full lines — experiment with isolated adsorber; dashed lines — calculated according to nonequilibrium model for different values of the parameter of heat accumulation and parameter KS of the rate equation (*11*) (given in Table 3).

The steepness of break-through curve corresponding to the nonequilibrium model depends on magnitude of the resistance against mass transfer the measure of which is the parameter KS in eqn (*11*). As obvious in Fig. 5, the consistence of the measured and calculated (dotted line) break-through curve is excellent in the lower section of the break-through curve whereas considerable deviations appear in the upper section. These differences are to be attributed to the incorrectly appraised value of heat loss. For higher values of heat loss the rate of supplementary saturation would be greater and simultaneously it would decrease more rapidly, which should manifest itself by approximation to the measured break-through

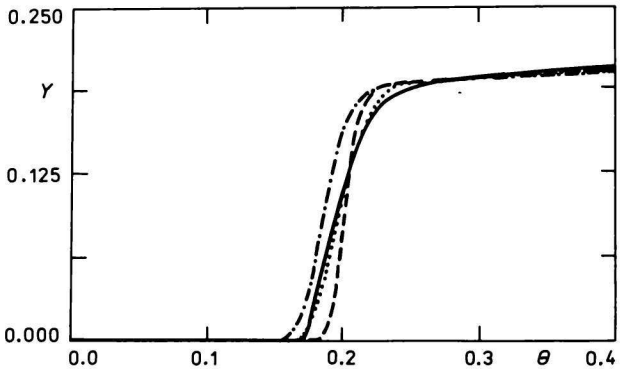

Fig. 7. Break-through curves; full line — experiment with nonisolated adsorber; dashed lines — calculated according to nonequilibrium model for different values of the parameters of heat accumulation and heat loss and parameter KS of the rate equation (*11*) (given in Table 3).

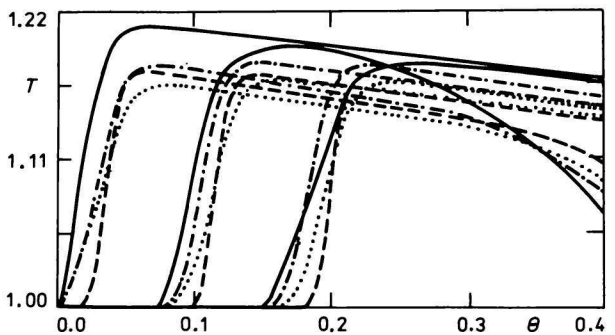

Fig. 8. Course of temperature in the first, second, and third part of adsorber; full lines — experiment with nonisolated adsorber; dashed lines — calculated according to nonequilibrium model for different values of the parameters of heat accumulation and heat loss and parameter KS of the rate equation (*11*) (given in Table 3).

curve. For the nonisothermal experiment (without isolation) the measured (full line) and calculated (dashed lines) break-through curves and temperature profiles are represented in Figs. 7 and 8. It results from Fig. 7 that the calculated break-through curves are distinguished by their position on the time axis and steepness. The different steepness ensues from the use of two different values of preexponential constant in the parameter of the equation of mass transfer (*4*). The shift in break-through curve along the axis of time is due to an increase in value of the parameter of heat accumulation as well as the parameter of heat loss while it can be observed from further progress of the calculated break-through curves that the rate of supplementary saturation is in all cases almost equal.

Conclusion

The presented equilibrium model of nonisothermal adsorption involves not only material and enthalpic balance but also a relatively complicated equilibrium relationship. The nonequilibrium model also includes the rate equation of mass transfer in the solid phase.

The prerequisite for good agreement of experimental and calculated results is the use of conveniently formulated equilibrium relationship including adequately expressed temperature dependence. As for the adsorption proceeding in laboratory conditions, we cannot omit in the model the term expressing the heat accumulation in walls or isolation of adsorber as well as the term regarding the heat losses. The terms of heat accumulation and heat losses significantly affect the results, especially at higher values of molar adsorption heat and relatively higher concentrations of adsorptive in the feed. These terms do not have such significant influence on modelling industrial adsorption because the diameter of industrial adsorbers is large and the heat capacity of walls and isolation is small with respect to the heat capacity of adsorbent. The presented results make evident that the inclusion of the rate of solid phase mass transfer into the model significantly contributes to achieving good agreement of the measured and calculated breaking time.

Symbols

a	preexponential constant for calculation of the diffusion coefficient	$m^2\ h^{-1}$
A	dimensionless constant in equilibrium relationship	
A_1	constant in equilibrium relationship	$mol\ kg^{-1}$
b	constant in exponent of the equation for calculation of the diffusion coefficient K	K
B	dimensionless constant in equilibrium relationship	
B_1	constant in equilibrium relationship	K^{-1}
c_{pb}	specific heat capacity of adsorbent	$kJ\ kg^{-1}\ K^{-1}$
c_{pg}	specific heat capacity of gas	$kJ\ kg^{-1}\ K^{-1}$
c_{pi}	specific heat capacity of isolation	$kJ\ kg^{-1}\ K^{-1}$
c_{ps}	specific heat capacity of the wall of adsorber	$kJ\ kg^{-1}\ K^{-1}$
CP	dimensionless specific heat capacity of gas	
CPS	dimensionless specific heat capacity of the wall of adsorber	
d_1	internal diameter of adsorber	m
d_2	external diameter of adsorber	m
d_3	external diameter of isolation, $d_3 = d_2$ for adsorber without isolation	m

D	dimensionless constant in equilibrium relationship	
D_1	constant in equilibrium relationship	$K^{-1/2}$
D_2	ratio of external and internal diameter of adsorber	
D_{ef}	effective diffusion coefficient	$m^2\ h^{-1}$
DH	dimensionless adsorption heat	
E	dimensionless porosity	
(ΔH)	molar adsorption heat	$kJ\ kmol^{-1}$
K_s	coefficient of mass transfer in the solid phase	h^{-1}
KS	dimensionless coefficient of mass transfer in the solid phase	
k_t	coefficient of heat transfer	$kJ\ m^{-2}\ h^{-1}\ K^{-1}$
KT	dimensionless coefficient of heat transfer	
M_2	molecular mass of nitrogen	$kg\ kmol^{-1}$
$M(CO_2)$	molecular mass of carbon dioxide	$kg\ kmol^{-1}$
$\bar{M}$	molecular mass of gas	$kg\ kmol^{-1}$
m_{Ms}	mass of adsorbent	kg
$\dot{n}_2$	molar flow of nitrogen	$kmol\ m^{-2}\ h^{-1}$
p_b	pressure in laboratory	kPa
r	radius of adsorbent particle	m
R	dimensionless constant in equilibrium relationship	
R_1	constant in equilibrium relationship	K
R2	dimensionless density of nitrogen	
RO	dimensionless density of gas	
RS	dimensionless density of adsorber wall	
t	time	h
T	dimensionless temperature	
T_g	temperature of gas	K
T_{g0}	temperature of the gas entering adsorber	K
T_{gi}	temperature of gas in adsorber at the start of the process	K
T_f	temperature of environment of adsorber	K
TF	dimensionless temperature of environment of adsorber	
T_m	temperature in laboratory	K
v	parameter respecting heat accumulation in isolation defined by eqn (*17*); $v = 1$ for adsorber without isolation	
x	relative fraction of adsorbate	$kmol\ kg^{-1}$
x^*	equilibrium relative fraction of adsorbate	$kmol\ kg^{-1}$
X	dimensionless relative fraction of adsorbate	
X^*	dimensionless equilibrium relative fraction of adsorbate	
Y	dimensionless relative fraction of adsorptive	
Y_g	relative mole fraction of adsorptive	$kmol\ kmol^{-1}$
Y_{g0}	relative mole fraction of adsorptive entering adsorber	$kmol\ kmol^{-1}$
Y_{gi}	relative mole fraction of adsorptive in adsorber at the start of the process	$kmol\ kmol^{-1}$
z	longitudinal coordinate	m
z_0	length of adsorbent bed	m

Z	dimensionless longitudinal coordinate	
ZC	dimensionless heat capacity of system	
α_k	combined coefficient of heat transfer by convection and radiation	kJ m^{-2} h^{-1} K^{-1}
α_p	coefficient of heat transfer by convection	kJ m^{-2} h^{-1} K^{-1}
α_r	coefficient of heat transfer by radiation	kJ m^{-2} h^{-1} K^{-1}
δ_i	width of isolation	m
δ_s	width of adsorber wall	m
ε	porosity of adsorbent bed	
λ_i	thermal conductivity of isolation	kJ m^{-1} h^{-1} K^{-1}
λ_s	thermal conductivity of adsorber wall	kJ m^{-1} h^{-1} K^{-1}
π	overall pressure in adsorber	Pa
ϱ_b	bulk density of adsorbent	kg m^{-3}
ϱ_g	density of gas	kg m^{-3}
ϱ_i	density of isolation	kg m^{-3}
ϱ_s	density of adsorber wall	kg m^{-3}
ϱ_2	density of nitrogen	kg m^{-3}
ϑ_f	temperature of environment	°C
ϑ_w	temperature of wall	°C
Θ	dimensionless time	

References

1. Kapusta, T., *CSc. Thesis.* Slovak Technical University, Bratislava, 1984.
2. Bobok, D., Kapusta, T., Kossaczký, E., and Hlavatý, T., *Ropa Uhlie 22*, 113 (1980).
3. Glueckauf, E., *Trans. Faraday Soc. 51*, 1540 (1955).
4. Hashimoto, K. and Miura, K., *J. Chem. Eng. Jap. 9*, 388 (1976).
5. Slavíček, E., *Teoretické základy chemického inženýrství.* (Theoretical Foundation of Chemical Engineering.) Státní nakladatelství technické literatury (State Publishing House of Technical Literature), Prague, 1969.
6. Bobok, D., Kossaczký, E., and Báleš, V., *Chem. Zvesti 34*, 589 (1980).
7. Kossaczký, E. and Surový, J., *Chemické inžinierstvo I.* (Chemical Engineering I.) Slovenské vydavateľstvo technickej literatúry (Slovak Publishing House of Technical Literature), Bratislava, 1964.

Translated by R. Domanský